# 23rd EUROPEAN ROTORCRAFT FORUM

Paper No. 91

# DYNAMIC ENGINE MODEL
# INTEGRATED IN HELICOPTER SIMULATION

by

M. Hamers,  W. von Grünhagen

September 16 - 18, 1997

Dresden

Germany

# Dynamic engine model integrated in helicopter simulation

M. Hamers
W. von Grünhagen
Deutsche Forschungsanstalt
für Luft- und Raumfahrt e.V. (DLR)
Institut für Flugmechanik
Braunschweig, Germany

## Abstract

An extensive physical based engine-governor-drive train model is integrated into the DLR helicopter simulation code SIMH. For that purpose, the main rotor formulation comprising rigid lead/lag and flap degrees of freedom is resolved for rotor speed and drive train dynamics. Parameterized engine and governor models are evaluated from complex high order physical descriptions, using reduction schemes, while still being physical meaningful, allowing for application in real time conditions. The full non-linear formulation is appropriate for the use in ground based simulation, allowing to cover the whole helicopter operative flight envelope.

The parameters of the reduced lower order models were optimized by comparing the simulation results with BO105 flight test data in hover and forward flight. With the inclusion of both engine and drive train dynamics, improvements in the dynamic prediction of helicopter shaft torque, rotor speed, heave and yaw motion for collective and pedal inputs could be achieved.

## Introduction

An important goal of helicopter simulation and modeling is a realistic prediction of dynamic response to control inputs in comparison with flight. In general, a modular structure dividing the helicopter model in components describing physical behaviour by non-linear or mathematical models, is used. This allows both componentwise validation and simple reconfiguration of single elements, when applied for simulator purposes. Through a process of stepwise increasing the component model's complexity and refining the description of physical dependencies an improvement in dynamic response prediction can be achieved.

The helicopter simulation code SIMH at DLR is described in detail in [1]. Here several model approaches

in the field of global and local rotor aerodynamics were investigated to improve the prediction of coupling behaviour, especially with respect to pitch⇔roll crosscoupling. The described extensions are taken as standard for subsequent investigations, which were recently focused on the field of rotor speed and engine dynamics. One objective is the elimination of the influence of engine dynamics on the yaw response, both for the on-axis response due to pedal inputs and for the off-axis response due to other control inputs. The model developed shall replace the empirical engine model described in [2].

Without engine dynamics the SIMH model performs well in predicting roll and pitch responses for cyclic control inputs. However, yaw response due to pilot collective or pedal control inputs shows more serious deficiencies in comparison to flight test data. To get an idea of the influence of engine and rotor speed dynamics on yaw rate prediction an open loop simulation, where measured shaft torque is fed into simulation, was performed. In forward flight regimes an improvement can be obtained. For these cases a correct simulation of engine and rotor speed dynamics seems to play a major role in improving the prediction of helicopter yaw behaviour. In hover however, for an open loop on shaft torque, the yaw rate improvement is less significant. From **figure 1** it can be seen that in the case of an ideal shaft torque prediction (open loop feed back) for a helicopter in hover the yaw rate improves only slightly. Especially after the pilot's correcting cyclic control input at about 6 sec., besides the engine dynamics the influence of other effects seems to be of importance. It is most likely that these effects have to be sought in the field of aerodynamic interferences of main rotor downwash on body and tail components. Because of the constant rotor speed in the closed loop simulation, all aerodynamic inputs directly affect shaft torque. Transient shaft torque prediction therefore diverges extensively from measured flight test data. Also in literature and recent publications [3], [4] it is shown that inclusion of dynamic engine modeling contributes to the increase of helicopter on- and off-axis prediction capability.
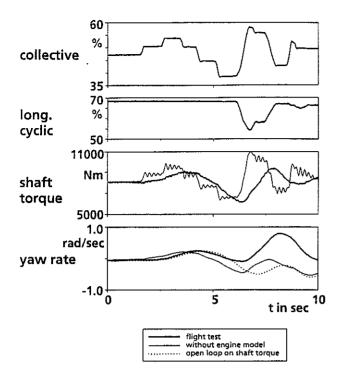
**Figure 1:** response to a 3-2-1-1 collective input in hover

Thus for both, forward speed and hover it is an interesting goal to improve engine and rotor speed dynamics behaviour in order to improve yaw response and to get a more clear insight of the remaining deficiencies in hover. The first approach to apply engine and rotor speed dynamics to the SIMH simulation code
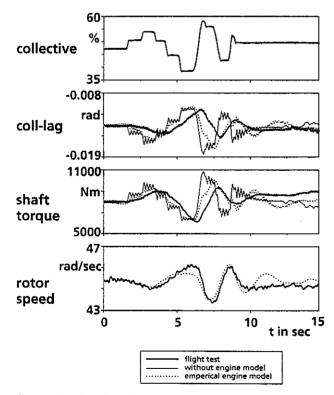


**figure 2:** closed and open loop yaw rate prediction for a 3-2-1-1 collective input in hover

was made by Gray and von Grünhagen [2]. An empirical linearized first order engine model in combination with a PID governor was implemented. In terms of rotor speed calculation the rotor was assumed to be a solid disk with a certain constant inertia. The resulting rotor speed equation was governed by the difference in engine torque on one hand and main and tail rotor torque on the other hand. Sets of optimized parameters were obtained from flight test data. Validation by means of detailed measurement data shows satisfactory rotor speed prediction but deficiencies in main rotor shaft torque and lead/lag motion, as depicted by the dashed lines in **figure 2** for the same hover case as displayed in figure 1. Collective lag is a multi-blade variable concerning lag motion equivalent to the coning variable for flap.

In this paper a dynamic engine model is presented that takes into account the interaction of the dynamics of all components included in the drive system and their feed back coupling to helicopter body motion.

## Dynamic engine modeling

Evaluating drive train torque equilibrium and considering the mechanical coupling of all elements, a differential equation for rotor speed can be defined. The obtained explicit formulation (i.e. equations resolved for rotor and lead/lag accelerations) causes in contrast to the implicit formulation of the existing empirical models less numerical problems and improves transient rotor dynamics. For substituting the shaft torque in the rotor speed equation the main rotor module of SIMH was reformulated by resolving the corresponding set of equations for rotor accelerations. The evaluated rotor angular acceleration was subsequently substituted in the respective components to calculate their coupling to the helicopter body through the resulting reaction forces and moments.

### Rotor speed equation

The various rotors and other drive train components as engine(s) and gearbox(es) mounted on a helicopter are mostly mechanically connected. Neglecting the elastic and therefore dynamic influence of the drive shaft torsion, the several appearing angular speeds are assumed to be proportional to each other, as illustrated in **figure 3**.

Normalizing all moments on main rotor speed the torque equilibrium then can be formulated as follows:

$$Q_{eng} - Q_{mr} - Q_{hub} - Q_{tr} - Q_{comp,j} - Q_{fric} = 0. \qquad (1)$$

with:

$$Q_k = C_k \cdot N_k \text{ and } C_k = \frac{\Omega_k}{\Omega_{mr}}, \qquad (2)$$

where $N_k$ is the resulting reaction moment evaluated from the respective submodel. The $Q_{comp}$ terms take account for additional aggregates as far as they are not already considered in the friction term. All moments $N_k$ can be separated in components that are dependent on absolute angular acceleration (the inertia terms) and terms that are not, here denoted as "static" moment:

$$N_k = \hat{N}_k + (\dot{\Omega}_k - \ddot{r}_{B,k}) \cdot I_k , \qquad (3)$$

where $\ddot{r}_{B,k}$ is the absolute body acceleration in the direction of rotation $\Omega_k$ of the particular component. However, only for the main rotor motion the $\ddot{r}_{B,mr}$-term (with $\ddot{r}_{B,mr} = \ddot{r}_{fs}$) is assumed to be of importance. For all other components body acceleration is neglected in comparison to $\dot{\Omega}_k$, thus:

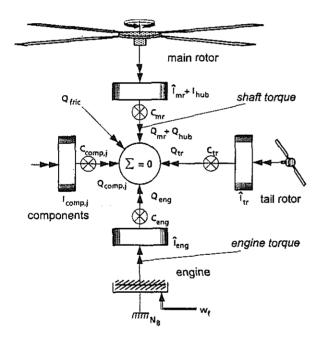$$(\dot{\Omega}_k - \ddot{r}_{B,k}) \approx \dot{\Omega}_k .$$



**Figure 3:** schematic torque equilibrium

Substituting equation (2) and (3) we obtain:

$$\dot{\Omega}_{mr} \cdot \left( n_{eng} \cdot C_{eng}^2 \cdot \hat{I}_{eng} + \hat{I}_{mr} + I_{hub} + C_{tr}^2 \cdot I_{tr} + C_{comp,j}^2 \cdot I_{comp,j} \right)$$

$$- \ddot{r}_{fs} \cdot (\hat{I}_{mr} + I_{hub}) = \qquad (4)$$

$$= n_{eng} \cdot C_{eng} \cdot \hat{N}_{eng} - \hat{N}_{mr} - C_{tr} \cdot \hat{N}_{tr} - C_{comp,j} \cdot \hat{N}_{comp,j} - N_{fric}$$

where $n_{eng}$ is the number of engines. When $n_{eng} > 1$ (f.e. BO105: $n_{eng} = 2$) the engines are assumed to show identical dynamic behaviour, although in reality a considerable difference in dynamics between the particular engines can occur.

To solve the above equation for rotor speed, all appearing static-moment and inertia terms have to be calculated from the several sub-models.

### Allison 250 C20 engine

The BO105 research helicopter at DLR is powered by two Allison 250 C20 B engines, which are twin shaft gasturbine engines with free running gas generator turbines. The power turbine is mechanically linked with the helicopter rotor drive through a gearbox. The engine is controlled by a dual-governor system, regulating fuel flow in dependence of both rotor speed (gas generator and power turbine) and compressor outlet pressure. Also a feed forward of pilot collective control setting is provided. Under normal flight conditions power turbine rotor speed is governed to the "100% $n_2$"-point (6016 rpm), corresponding with a main rotor speed of 44.4 rad/s for the BO105 helicopter.

The engine is modeled by a linearized second order state space model [5,6], which is derived from a sophisticated 22nd order fully non-linear model, describing all necessary engine dynamic and thermodynamic quantities. The obtained second order model

$$\begin{pmatrix} \dot{n}_1 \\ \dot{n}_2 \end{pmatrix} = \begin{bmatrix} -\dfrac{1}{\tau_1} & 0 \\ k_2 & -\dfrac{1}{\tau_2} \end{bmatrix} \cdot \begin{pmatrix} n_1 \\ n_2 \end{pmatrix} + \begin{pmatrix} k_1 \\ k_3 \end{pmatrix} \cdot w_f - \begin{pmatrix} 0 \\ k_4 \end{pmatrix} \cdot N_{eng} , \quad (5)$$

only accounting for the power and gas turbine inertia, is a good approximation of the dynamic engine as a function of fuel flow and external moment and is therefore well suited for application in helicopter (real time) simulation.

After short reformulation from equation (5) the differential equations for gas generator ("1") speed and power turbine ("2") moment are obtained:

$$\dot{n}_1 = -\frac{1}{\tau_1} \cdot n_1 + k_1 \cdot w_f \qquad (6)$$

and

$$N_{eng} = -\frac{1}{k_4} \cdot \dot{n}_2 - \frac{1}{k_4 \cdot \tau_2} \cdot n_2 + \frac{k_2}{k_4} \cdot n_1 + \frac{k_3}{k_4} \cdot w_f \qquad (7)$$

or in short notation, allowing direct substitution in equation (4):

$$N_{eng} = -\hat{I}_{eng} \cdot \dot{\Omega}_{eng} + \hat{N}_{eng} \qquad (8)$$

with $\hat{I}_{eng} = \dfrac{C_{rad/s \to \%}}{k_4}$ .

From equation (6) we can see, that the $n_1$ rotor speed and herewith the produced amount of gas is directly governed by the fuel flow. The engine torque again is linear dependent on the produced gas flow and thus on $n_1$ rotor speed. The direct dependence of rotor torque on thermal gas flow energy supplied by the fuel injection, is expressed by the third term in equation (7). The torque increase or decrease for external rotor slow down or speed up, respectively is considered in the second term. Finally the factor $1/\bar{k}_4^*$ is directly correlated with the power turbine inertia.

The engine coefficients $k_1$ to $k_3$ and $\tau_1$ and $\tau_2$ were evaluated from engine test bed results. In [6] these parameters are listed as a function of the gas producer rotor speed $n_1$, which can be determined from the steady state engine torque diagram in dependence of engine torque, as shown in **figure 4**.
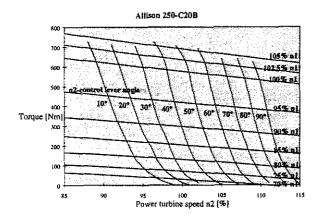
Allison 250-C20B

Figure 4: engine performance

The factor $\bar{k}_4$ is also identified from test bed investigations. Because of the test bed configuration, where a power brake was directly mounted on the engine shaft, $\bar{k}_4$ corresponds with the total inertia of power turbine and brake. In $\bar{k}_4^*$ however, only the power turbine inertia has to be taken into account. At DLR no information on the engine inertia was available. Therefore engine speed-up investigations with a BO105 spare engine were performed [7] to determine the $n_2$-inertia on an experimental way.

## Governor

The Allison 250 C20B is controlled by a pair of hydro-mechanical governors. The $n_1$-governor directly controls the fuel flow in dependence of $n_1$-rotor speed, the power setting by the pilot (throttle) and an adjustable $n_1$-command speed setting, which is directly controlled by the $n_2$-governor output signal. The $n_1$-governor is mainly active during engine start-up and shut-down procedures. In level flight the $n_2$-governor provides the main influence on fuel supply. To avoid strong deviations of

main rotor speed from the trim speed in flight maneuvers requiring strong engine power changes, such as collective inputs, additionally a feed forward of the pilot's collective pitch control is realized.

The components in this hydro-mechanical structure show strong non-linear behaviour. An approach was made to derive the most significant effects from this complex structure, which is illustrated in **figure 5**:
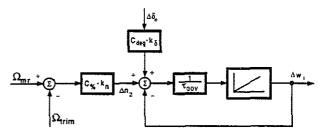
**Figure 5:** governor modeling

The control law for fuel flow in dependence of rotor speed deviation is assumed to be a PT governor, D- and I-terms were omitted. Also the feed forward structure controlling fuel flow directly by pilot collective inputs is considered. The remaining governor coefficients are subject to a parameter optimization by matching flight test data in the time domain. The optimization was conducted for hover collective 3-2-1-1 inputs.

The factors $C_{\%}$ and $C_{\delta c_g}$ account for the transformation of [rad/s] to [%] and of collective pitch change in [%] to governor pitch lever angle in [rad].

## Main rotor with lead/lag and flap

The four bladed hingeless rotor of the BO105 helicopter is modeled by an equivalent hinge-spring-damper system for lead/lag and flap degrees of freedom. In the appendix a reduction of the main rotor shaft torque equation is performed onto a formulation defined by equation (3). Apart from the absolute angular acceleration all rotor accelerations are eliminated. According to equation (A15) the shaft moment can be expressed like:

$$N_{mr} = \hat{N}_{mr} + \left(\dot{\Omega}_{mr} - \dot{r}_{fs}\right)\cdot\left(\hat{I}_{mr} + I_{hub}\right) , \qquad (9)$$

which can directly be substituted in the rotor speed equation (4). The equivalent main rotor inertia $\hat{I}_{mr}$ described in (9) is according to (A14) a pure constructional parameter:

$$\hat{I}_{mr} = n_i \cdot e_i^2 \cdot \left(m_B - \frac{M_B^2}{I_B}\right) , \qquad (10)$$

which is much less than the inertia of the same rotor considered with rigid blades. For example the equivalent

inertia for a BO105 rotor is about $\bar{I}_{mr} \approx 14$ kgm$^2$, which is one order of magnitude less than the comparable rigid rotor inertia. Because of the blade degrees of freedom about the hinge the rotor blades can show higher instantaneous dynamics separate from the rotor inner part and drive train, making the whole system less stiff.

The rotor acceleration equation however, is resolved for the relative acceleration $\dot{\Omega}_{mr}$ rather than the absolute one listed in equation (9). To eliminate the body acceleration $\ddot{r}_{fs}$ in the appendix a second relation between body and rotor acceleration is evaluated (A19):

$$\ddot{r}_{fs} = F'_{\Sigma} + \left(\dot{\Omega}_{mr} - \ddot{r}_{fs}\right) \cdot \frac{\hat{I}_{mr} + I_{hub}}{\hat{I}_{s,z}} . \qquad (11)$$

The term in the denominator denoted as the equivalent body inertia $I_{s,z}$ is in the same order of magnitude as the helicopter yaw inertia and thus more than two orders of magnitude higher than the sum of main rotor equivalent inertia and hub inertia. It is therefore assumed that the friction in equation (11) is negligible small in comparison to the "static" terms. The body acceleration can now easily be substituted in the rotor speed equation.

When the drive train angular acceleration is calculated substituting equations (3), (8) and (9) in the rotor speed equation it is subsequently substituted in equation (A8) and (A9) to determine lead/lag and flap motion.

## Tail rotor and other components

The blades of the BO105 teetering tail rotor are much stiffer in comparison to the main rotor blades. Therefore no equivalent lagging system is considered and thus no extra degrees of freedom in rotational direction are introduced. The tail rotor inertia is purely determined from the rotating solid blade and hub masses. The "static" moment is calculated from the aerodynamic conditions at the tail rotor. The tail rotor torque can then be expressed like:

$$N_{tr} = N_{tr,aero} + I_{tr} \cdot \dot{\Omega}_{tr} = \hat{N}_{tr} + I_{tr} \cdot \dot{\Omega}_{tr}. \qquad (12)$$

Similar approaches are made for other components as gearboxes and aggregates:
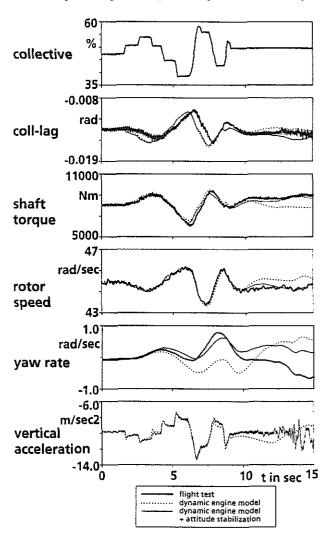
$$N_{comp,j} = \hat{N}_{comp,j} + I_{comp,j} \cdot \dot{\Omega}_{comp,j} , \qquad (13)$$

where required torque and respective inertia are constructional factors. Friction is assumed as a "static" moment, only dependent on engine torque and rotor speed, not affecting drive train dynamics.

## Coupling to helicopter body

When the drive train dynamics are formulated in the explicit way described before, then the coupling moment to the helicopter body about a particular axis is the sum of all external moments (mostly of aerodynamic origin) and all inertia terms about that axis. The inertia terms of the rotating components are calculated from equation (3) by substituting the rotor angular acceleration. When f.e. besides the rotor and hub inertia no further inertia about the z-axis are assumed, the total coupling moment through main rotor on the fuselage is equivalent to the shaft moment $N_{fs,z}$ in equation (A14). In x-direction only the *inertia* terms of engine and other possible components couple to the helicopter body. Engine torque is an internal moment and thus not considered as coupling moment.

## Results

Validation of the dynamic engine model requires flight test date providing rotor speed, engine or shaft torque



**Figure 6:** response to collective 3-2-1-1 input in hover

and collective lag, which is a multi blade variable for lag motion equivalent to the coning variable for flap. At DLR a flight test data base for the BO105 helicopter exists.
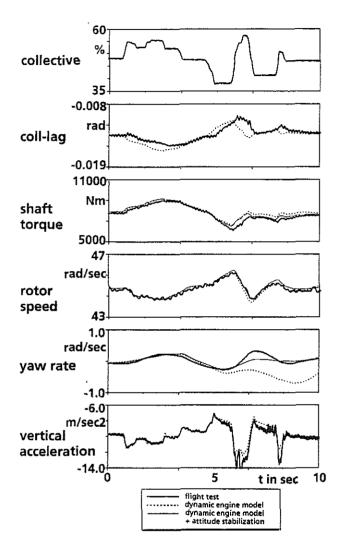


Figure 7: response to collective 3-2-1-1 input in hover

The performance of the dynamic engine model for a collective 3-2-1-1 control input in hover is shown in figure 6 and figure 7. Major improvements in shaft torque and rotor speed can be lined out, when figure 6 compared with figure 1. Also collective lag prediction improves when compared to figure 2. The transient lag oscillations as response to collective control input, shown in figure 1 for existing models, seems to be washed out by the dynamic engine. This effect is due to the decreased inner rotational stiffness, inherent to the explicit acceleration formulation. The occurring time shift is possibly due to unmodeled sensor dynamics or the simplification made by lead/lag equivalent hinge system affect the collective lag match. The simulated on-axis response in heave shows good fit for both cases. For the off-axis yaw response the fact described for figure 1

occurs: when shaft torque is predicted well, still deficiencies in yaw dynamics remain. Unmodeled aerodynamic effects and the pilot's correcting inputs in cylic and pedal controls after about 6 seconds in both cases cause drifts in the helicopter pitch and roll attitude. The yaw response can further be improved, when the attitude is stabilized in pitch and roll, by the use of inverse simulation [9]. The thin lines in figures 6 and 7 display, that engine dynamics are only slightly affected when the attitude stabilization is performed.

In figure 8 the simulation performance for a collective 3-2-1-1 input at 80 kts forward speed is shown. Because of the more stable attitude at 80 kts, here no stabilization is performed. The engine torque from simulation is compared with the indicated measured engine torque. Again good results for the rotor and engine dynamics and the on-axis heave response are obtained. Also improvement in yaw prediction, especially in the yaw response magnitude is achieved.
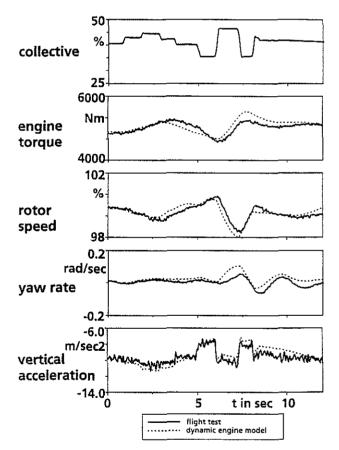


Figure 8: response to a collective 3-2-1-1 input at 80 kts

Figure 9 shows the simulation of a collective sinusoidal input also at 80 kts forward speed. Engine and rotor dynamics fit well with the measured dynamic behaviour. In the on- and off-axis response slight deviations occur due to a low frequency oscillation in pitch attitude affecting yaw rate and heave motion.
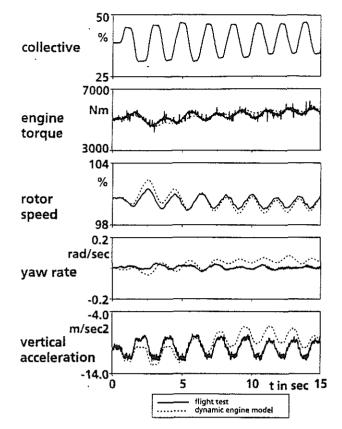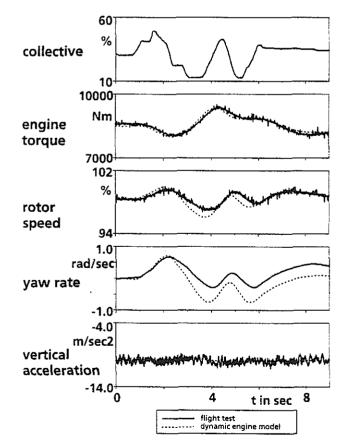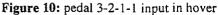
Figure 9: sinusoidal collective input at 80 kts



Figure 10: pedal 3-2-1-1 input in hover

Finally to check the on-axis response of pedal input on yaw rate for hover a pedal 3-2-1-1 input is simulated. The responses are illustrated in **figure 10**. Hover attitude is not stabilized, which causes slow attitude drifts affecting the on-axis yaw response.

## Conclusions

A nonlinear engine-governor-drive train model is developed and integrated in the SIMH helicopter simulation code. The physically based explicit formulation of the engine and rotor dynamics makes it suitable for the application in ground based helicopter simulation, for example DLR's new ACT/FHS simulator. The engine and governor were simulated by parameterized linear models, derived from complex physical high order model structures. Engine coefficients were taken from test bed results, whereas governor coefficients were optimized by comparing the predicted overall model responses for collective inputs with flight test data in hover.

A fairly improved approximation of main rotor shaft torque cq. engine torque and rotor speed could be achieved. The predicted on-axis response for collective control input to heave and pedal control input to yaw also show very good correlation with the measured flight data. In the off-axis response prediction, especially yaw due to collective control, improvements have been made, although deficiencies remain. They are most likely due to aerodynamic interferences of main rotor downwash and vorticities on tail components. The improved engine and drive train dynamics, however, allow a more precise and accurate determination of these remaining effects in future investigations.

## References

[1] M. Hamers, W. von Grünhagen
"Nonlinear Helicopter Model Validation Applied to Realtime Simulation"
AHS 53rd Annual Forum, May 1997, Virginia Beach Virginia
[2] G. Gray, W. von Grünhagen
"An Investigation of Open Loop and Inverse Simulation as Nonlinear Model Validation Tools for Helicopter Flight Mechanics"
Conference on Rotorcraft Simulation, May 1994, London
[3] G. D. Padfield
"Helicopter Flight Dynamics"
Blackwell Science Ltd, 1996, Oxford

[4]  J. W. Fletcher, M. B. Tischler
"*Improving Helicopter Flight Mechanics Models with Laser Measurements of Blade Flapping*"
AHS 53rd Annual Forum, May 1997, Virginia Beach, Virginia
[5]  G. Kappler, W. Erhard and M. Menrath
"*Application of an Extended Dynamic Engine Model to the Helicopter Engine Allison 250-C20*"
Technische Universität München, 1990, Munich
[6]  M. Menrath
"*Experimentelle Kennwertermittlung und Systemanalyse bei Hubschrauber-Gasturbinen*"
Technische Universität München, 1995, Munich
[7]  M. Hamers
"*Inertia Measurement of the  Allison 250 C20B Engine*"
IB 111-97/05
German Aerospace Research Establishment
Institute of Flight Mechanics, 1997, Braunschweig. (in German)
[8]  W. von Grünhagen
"*Helicopter Modelling and Simulation, Mathematical Description*"
IB 111-88/06
Institute of Flight Mechanics, 1988, DLR Braunschweig (in German)

# Appendix

In this appendix a short overview is given how the equation for the resulting main rotor shaft moment is resolved for rotor absolute angular acceleration terms. The reaction moment is seperated into acceleration dependent and non-dependent components. In the moment equation, however, not only rotor speed- but also flap and lead/lag-acceleration appear. The respective flap and lead/lag differential equations are also resolved for rotor speed acceleration and then substituted in the moment equation.

Because the rotor speed equation is resolved for the relative (to helicopter body) angular rotor acceleration and not for the absolute acceleration, in order to eliminate body acceleration terms, a further relation between the respective accelerations is needed, which is obtained by resolving the helicopter rotational equations.

## Nomenclature

| | |
|---|---|
| a | acceleration [m/s$^2$] |
| c | spring constant [Nm/rad] |
| d | damper constant [Nms/rad] |
| $d_i$, $e_i$, $f_i$ | hinge displacement [m] |
| k | engine and governer coefficients [-] |
| m | mass [kg] |
| n | number [-] |
| n | engine rotor speed [%] |

| | |
|---|---|
| p, q, r | angular rates [rad/s] |
| r | displacement [m] |
| u, v, w | velocities [m/s] |
| w | flow [g/s] |
| C | speed ratio [-] |
| F | force [N] |
| I | inertia [kgm$^2$] |
| M | first mass moment ([kgm] |
| N | moment [Nm] |
| Q | torque normalized on main rotor speed [Nm] |
| R | main rotor radius [m] |
| $\beta, \zeta$ | flap and lag angles [rad] |
| $\delta$ | pilot control input [%] |
| $\rho$ | radial displacement [m] |
| $\tau$ | time constant [s] |
| $\varphi, \vartheta, \psi$ | rotor tilt and azimuth angles [rad] |
| $\omega$ | relative coordinate system rotation [rad/s] |
| $\Omega$ | angular speed [rad/s] |

## Indices

| | |
|---|---|
| aero | aerodynamic |
| be | blade element coordinate system |
| bl | blade |
| bs | blade span coordinate system |
| c | collective pitch |
| comp | drive train component |
| e | hinge coordinate system |
| eng | engine |
| f | fuel |
| fin | fin |
| fs | fixed shaft coordinate system |
| fus | fuselage |
| fric | friction |
| gov | governor |
| hub | hub coordinate system |
| i | blade |
| k | submodel |
| mr | main rotor |
| rs | rotating shaft coordinate system |
| tr | tail rotor |
| x, y, z | axis |
| B | body coordinate system |

## Main rotor equivalent hinge system

The main rotor model in SIMH describes a four bladed rotor with equivalent hinge-spring-damper systems for flap and lead/lag DOF. For the engine dynamics investigations a version with coincident flap and lead/lag hinges is taken. The blades are divided in several blade elements. The aerodynamics are calculated for each blade and element separately.

The overall SIMH is not fully resolved for all appearing accelerations but makes use of a mixed implicit description, where rotor equations contain body accelerations and vice versa. The integration scheme is slightly modified to minimize the influence of this fact.

Except for body accelerations the rotor model itself is formulated explicitly for all accelerations, as there are lead/lag, flap and rotor anglar acceleration.
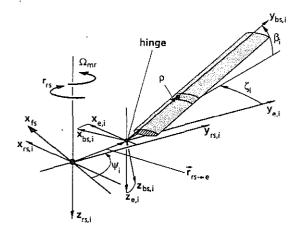


**figure 1:** schematic set up of main rotor model

Figure 1 shows schematically the transformations to be performed from fixed shaft to blade span system. For velocities and accelerations in both translatory and rotational direction the following vector definitions are used:

$$\vec{v} = \begin{pmatrix} u \\ v \\ w \end{pmatrix}, \quad \vec{p} = \begin{pmatrix} p \\ q \\ r \end{pmatrix}, \quad \vec{a} = \begin{pmatrix} a_x \\ a_y \\ a_z \end{pmatrix} \quad \text{and} \quad \dot{\vec{p}} = \begin{pmatrix} \dot{p} \\ \dot{q} \\ \dot{r} \end{pmatrix},$$

and for forces and moments: $\vec{F} = \begin{pmatrix} F_x \\ F_y \\ F_z \end{pmatrix}$ and $\vec{N} = \begin{pmatrix} N_x \\ N_y \\ N_z \end{pmatrix}$

respectively.

## Accelerations at the blade element

To evaluate lead/lag and resulting shaft moment equations the absolute acceleration terms at the blade element have to be calculated. For this, states and state derivatives are transformed from body cg. to blade element taking into account all appearing degrees of freedom between cg. and blade element. The rotor angular acceleration appears in the transformation from fixed to rotating shaft system:

$$\vec{v}_{rs,i} = [A_\varphi]_i \cdot \vec{v}_{fs} ,$$
$$\vec{p}_{rs,i} = [A_\varphi]_i \cdot \vec{p}_{fs} - \Omega_{mr} \cdot (0,0,1)^T ,$$
$$\vec{a}_{rs,i} = [A_\varphi]_i \cdot \vec{a}_{fs} , \tag{A1}$$
$$\dot{\vec{p}}_{rs,i} = [A_\varphi]_i \cdot \dot{\vec{p}}_{fs} + [\dot{A}_\varphi]_i \cdot \vec{p}_{fs} - \dot{\Omega}_{mr} \cdot (0,0,1)^T ,$$

with

$$[A_v]_i = \begin{pmatrix} \sin\psi_i & \cos\psi_i & 0 \\ -\cos\psi_i & \sin\psi_i & 0 \\ 0 & 0 & 1 \end{pmatrix}.$$

From the above angular acceleration vector $\dot{\vec{p}}_{rs,i}$ the term $\dot{r}_{rs} = \dot{r}_{fs} - \Omega_{mr}$ , which stands for the absolute (i.e.

with respect to the inertial system) rotor acceleration, can be extracted:

$$\dot{\vec{p}}_{rs,i} = \dot{\vec{p}}'_{rs,i} + \dot{r}_{rs} \cdot (0,0,1)^T = \dot{\vec{p}}'_{rs,i} + \dot{\vec{\Omega}}_{abs} . \tag{A2}$$

The accent marks indicate that in the respective terms no further rotor accelerations are included. Subsequent transformation into the hinge system, for the case of coincident flap and lead/lag hinge gives:

$$\vec{v}_{e,i} = \vec{v}_{rs,i} + \vec{p}_{rs,i} \times \vec{r}_{rs \to e} ,$$
$$\vec{p}_{e,i} = \vec{p}_{rs,i} ,$$
$$\vec{a}_{e,i} = \vec{a}_{rs,i} + \dot{\vec{p}}_{rs,i} \times \vec{r}_{rs \to e} + \vec{p}_{rs,i} \times (\vec{p}_{rs,i} \times \vec{r}_{rs \to e})$$
$$\qquad = \vec{a}_{rs,i} + \dot{\vec{p}}'_{rs,i} \times \vec{r}_{rs \to e} + \vec{p}_{rs,i} \times (\vec{p}_{rs,i} \times \vec{r}_{rs \to e})$$
$$\qquad \quad + \dot{\vec{\Omega}}_{abs} \times \vec{r}_{rs \to e} \tag{A3}$$
$$\qquad = \vec{a}'_{e,i} + \dot{\vec{\Omega}}_{abs} \times \vec{r}_{rs \to e}$$
$$\dot{\vec{p}}_{e,i} = \dot{\vec{p}}_{e,i} = \dot{\vec{p}}'_{rs,i} + \dot{\vec{\Omega}}_{abs} ,$$

with $\vec{r}_{rs \to e} = (d_1, e_1, f_1)^T$ the hinge displacement vector.

Further rotation about lead/lag angle $\zeta_i$ and flap angle $\beta_i$ respectively leads to:

$$\vec{v}_{bs,i} = [A_{\beta\zeta}]_i \cdot \vec{v}_{e,i} ,$$
$$\vec{p}_{bs,i} = [A_{\beta\zeta}]_i \cdot \vec{p}_{e,i} + \vec{\omega}_{i,e \to bs} ,$$
$$\vec{a}_{bs,i} = [A_{\beta\zeta}]_i \cdot \vec{a}_{e,i} = \vec{a}'_{bs,i} + [A_{\beta\zeta}]_i \cdot (\dot{\vec{\Omega}}_{abs} \times \vec{r}_{rs \to e}), \tag{A4}$$
$$\dot{\vec{p}}_{bs,i} = [A_{\beta\zeta}]_i \cdot \dot{\vec{p}}_{e,i} + [\dot{A}_{\beta\zeta}]_i \cdot \vec{p}_{e,i} + \dot{\vec{\omega}}_{i,e \to bs}$$
$$\qquad = [A_{\beta\zeta}]_i \cdot \dot{\vec{p}}'_{e,i} + [\dot{A}_{\beta\zeta}]_i \cdot \vec{p}_{e,i} + [A_{\beta\zeta}]_i \cdot \dot{\vec{\Omega}}_{abs}$$
$$\qquad \quad + \dot{\vec{\omega}}'_{i,e \to bs} + \dot{\vec{\omega}}_{i,e \to bs,\zeta} \cdot \ddot{\zeta}$$
$$\qquad = \dot{\vec{p}}'_{bs,i} + [A_{\beta\zeta}]_i \cdot \dot{\vec{\Omega}}_{abs} + \dot{\vec{\omega}}_{i,e \to bs,\zeta} \cdot \ddot{\zeta}$$

with

$$[A_{\beta\zeta}]_i = \begin{pmatrix} \cos\zeta_i & -\sin\zeta_i & 0 \\ \cos\beta_i \sin\zeta_i & \cos\beta_i \cos\zeta_i & -\sin\beta_i \\ \sin\beta_i \sin\zeta_i & \sin\beta_i \cos\zeta_i & \cos\beta_i \end{pmatrix}$$

and $\vec{\omega}_{i,e \to bs} = (-\dot{\beta}_i, \dot{\zeta}_i \cdot \sin\beta_i, \dot{\zeta}_i \cdot \cos\beta_i)^T$.

The last vector describes the relative rotation between the hinge and the blade span coordinate system.

Finally, the linear transformation from blade span to blade segment system (bs→be) is defined by a similar set of equations as described in (A3) for the

transformation from rotating shaft to hinge system (rs→e). With a radial displacement vector of

$$\vec{r}_{hs \to he} = (0, \rho, 0)^T \quad \text{with} \quad 0 \le \rho \le (R - e_i) .$$

this results in the blade element acceleration $\vec{a}_{he,i}$

## Flap and lead/lag differential equation

The Newton equations defining hinge moment equilibrium between the inertia, aerodynamic and hinge spring and damper loads are used to derive flap- and lead/lag differential equations. For evaluating the $i^{th}$ flap and lead/lad differential equation, using Newton's law this equilibrium about the hinge is defined as:

$$\sum \vec{N}_i = \int (\vec{r}_{hs \to he} \times \vec{a}_{he,i}) \cdot dm . \qquad . \qquad (A5)$$

After substituting the blade element acceleration $\vec{a}_{he,i}$ the term on the right hand side can be analytically integrated from hinge to blade tip. Introducing:

$$m_{bi} = \int dm , \quad M_{bi} = \int \rho \cdot dm \quad \text{and} \quad I_{bi} = \int \rho^2 \cdot dm$$

as the blade mass, the blade first and second inertia moment about the hinge, differential equations for lead/lag and flap motion are evaluated from the x- and z-component of the obtained vector equation:

$$\ddot{\zeta}_i = -\frac{N_{aero\,i,z} + c_\zeta \cdot \zeta_i + d_\zeta \cdot \dot{\zeta}_i}{\cos\beta_i \cdot I_B}$$
$$-\frac{a'_{hs,i,z} \cdot M_B}{\cos\beta_i \cdot I_B} - \frac{p_{bs,i} \cdot q_{bs,i}}{\cos\beta_i} + \frac{\dot{r}'_{bs,i}}{\cos\beta_i} \qquad (A6)$$
$$+ \dot{r}_{rs} \cdot \left(1 + \frac{M_B}{I_B} \cdot \frac{e_i \cdot \cos\zeta_i + d_i \cdot \sin\zeta_i}{\cos\beta_i}\right)$$

for lag motion and:

$$\ddot{\beta}_i = -\frac{N_{aero\,i,x} + c_\beta \cdot \beta_i + d_\beta \cdot \dot{\beta}_i}{I_B}$$
$$+ a'_{hs,i,z} \cdot \frac{M_B}{I_B} + q_{bs,i} \cdot r_{bs,i} + \dot{p}'_{bs,i} \qquad (A7)$$
$$- \dot{r}_{rs} \cdot (e_i \cdot \sin\zeta_i - d_i \cdot \cos\zeta_i) \cdot \frac{M_B}{I_B} \cdot \sin\beta_i$$

for flap. When summarizing for rotor absolute angular acceleration dependent and non-dependent terms, equations (A6) and (A7) can be written in short notation:

$$\ddot{\zeta}_i = \frac{F'_{lag,i}}{\cos\beta_i} + \dot{r}_{rs} \cdot C_{lag,i} \qquad (A8)$$

and

$$\ddot{\beta}_i = F'_{flap,i} - \dot{r}_{rs} \cdot C_{flap,i} . \qquad (A9)$$

## Main rotor shaft moment

Blade dynamics and aerodynamics couple to the rotor shaft through the hinge reaction forces and moments:

$$\vec{N}_{rs,i} = \vec{N}_{e,i} + \vec{r}_{rs \to e} \times \vec{F}_{e,i}$$
$$= [A_{\beta,\zeta}]_i^{-1} \cdot \vec{N}_{hs,i} + \vec{r}_{rs \to e} \times \left([A_{\beta,\zeta}]_i^{-1} \cdot \vec{F}_{hs,i}\right) \qquad (A10)$$

The hinge moments result from blade motion and blade displacement:

$$\vec{N}_{hs,i} = \begin{pmatrix} -c_\beta \beta_i - d_\beta \cdot \dot{\beta}_i \\ N_{aero\,i,y} \\ -c_\zeta \cdot \zeta_i - d_\zeta \cdot \dot{\zeta}_i \end{pmatrix} , \qquad (A11)$$

whereas the hinge forces are evaluated from defining a Newton's force equilibrium between aerodynamic and inertia loads:

$$\sum \vec{F}_i = \sum \vec{F}_{aero,i} + (-\vec{F}_{hs,i}) = \int \vec{a}_{he,i} \cdot dm . \quad (A12)$$

Substituting the blade element accelerations and summarizing over the number of blades $n_i$ the total moment in shaft direction (rotor torque) is obtained as:

$$N_{\beta,z} = N_{rs,z} = \sum_i N_{rs,i,z}$$
$$= N'_{rs,z} - n_i \cdot \dot{r}_{rs} \cdot m_B \cdot (d_i^2 + e_i^2) \qquad (A13)$$
$$+ \sum_i [(\ddot{\zeta}_i - \dot{r}_{rs}) \cdot M_B \cdot \cos\beta_i \cdot (d_i \sin\zeta_i + e_i \cos\zeta_i)]$$
$$+ \sum_i [-\ddot{\beta}_i \cdot M_B \cdot \sin\beta_i \cdot (e_i \sin\zeta_i - d_i \cos\zeta_i)]$$

In this formulation besides the rotor acceleration also lead/lag and flap accelerations occur, which can be substituted by equations (A8) and (A9). When simultaneously a reduction by ordering scheme is performed under the assumption that the hinge displacement in x- and z-directions is small in comparison to the y-direction, i.e. $d_i$, $f_i \ll e_i$ , we finally obtain for the rotor torque:

$$N_{\beta,z} = N'_{rs,z} + (F'_{lag} - F'_{flap}) \cdot M_B \cdot e_i$$
$$- \dot{r}_{rs} \cdot n_i \cdot e_i^2 \cdot \left(m_B - \frac{M_B^2}{I_B}\right) \qquad (A14)$$

For the use in the rotor acceleration equation, also taking into account the main rotor hub inertia $I_{hub}$, we can write from (A14) in short notation:

$$N_{mr} = N_{fs,z} = \hat{N}_{mr} - \dot{r}_{rs} \cdot \left( \hat{I}_{mr} + I_{hub} \right)$$

$$= \hat{N}_{mr} + \left( \dot{\Omega}_{mr} - \dot{r}_{fs} \right) \cdot \left( \hat{I}_{mr} + I_{hub} \right) \tag{A15}$$

or in vector formulation:

$$\bar{N}_{fs} = \bar{N}'_{fs} - \dot{\bar{\Omega}}_{abs} \cdot \hat{I}_{mr} \ . \tag{A16}$$

The first three terms in (A14) are not dependent on absolute rotor acceleration, but only on rotor state variables. They are denoted as the main rotor "static" moment $\hat{N}_{mr}$. The constant inertia factor $\hat{I}_{mr}$ is interpreted as the main rotor equivalent inertia.

## Body equations of rotational motion

As mentioned before the body acceleration $\dot{r}_{fs}$ (expressed in fixed shaft coordinates) has to be eliminated from the rotor speed equation. Therefore a further relation between $\dot{r}_{fs}$ and $\dot{\Omega}_{mr}$ is evaluated from the body rotational equations:

$$\bar{N}_B = \bar{I}_B \cdot \dot{\bar{p}}_B + \bar{p}_B \times \bar{I}_B \cdot \bar{p}_B \ , \tag{A17}$$

where $\bar{I}_B$ is the body inertia tensor and $\bar{N}_B$ the sum of reaction moments of all particular components coupled to the helicopter body with respect to body cg.:

$$\bar{N}_B = \bar{N}_{B,mr} + \bar{N}_{B,tr} + \bar{N}_{B,fus} + \bar{N}_{B,fin} + \ldots \tag{A18}$$

The assumption is made that the inertia terms appearing in equation (A18) are neglifible small in comparison to the main rotor inertia. For a main rotor reaction moment coupled to the body of:

$$\bar{N}_{B,mr} = \left[ A_{\varphi,\vartheta} \right]^{-1} \cdot \bar{N}_{fs} + \bar{r}_{B,cg \to fs} \times \left( \left[ A_{\varphi,\vartheta} \right]^{-1} \cdot \bar{F}_{fs} \right) , \tag{A19}$$

with

$$\left[ A_{\varphi,\upsilon} \right] = \begin{pmatrix} \cos\vartheta & 0 & -\sin\vartheta \\ \sin\varphi \sin\vartheta & \cos\varphi & \sin\varphi \cos\vartheta \\ \cos\varphi \sin\vartheta & -\sin\varphi & \cos\varphi \cos\vartheta \end{pmatrix}$$

describing main rotor shaft tilt, the angular body acceleration expressed in fixed shaft coordinates:

$$\dot{\bar{p}}_{fs} = \left[ A_{\varphi,\vartheta} \right] \cdot \dot{\bar{p}}_B - \left[ A_{\varphi,\vartheta} \right] \cdot \left( \bar{I}^{-1} \cdot \left( \left[ A_{\varphi,\vartheta} \right]^{-1} \cdot \left( \dot{\bar{\Omega}}_{abs} \cdot \hat{I}_{mr} \right) \right) \right) .$$
$$\tag{A20}$$

is obtained.

When finally the z-component of the above equation is evaluated the desired relation between $\dot{r}_{fs}$ and $\dot{\Omega}_{mr}$ is given by:

$$\dot{r}_{fs} = F'_{rot} + \left( \dot{\Omega}_{mr} - \dot{r}_{fs} \right) \cdot \frac{\hat{I}_{mr} + I_{hub}}{\hat{I}_{B,z}} \ . \tag{A21}$$

The equivalent body inertia $I_{B,z}$ in the denominator of the last term is in the same order of magnitude as the body inertia about z-axis.